Optical Engineering

OpticalEngineering.SPIEDigitalLibrary.org

Indoor visible light communication localization system utilizing received signal strength indication technique and trilateration method

Farag I. K. Mousa
Noor Almaadeed
Krishna Busawon
Ahmed Bouridane
Richard Binns
Ian Elliot

SPIE.

Farag I. K. Mousa, Noor Almaadeed, Krishna Busawon, Ahmed Bouridane, Richard Binns, Ian Elliot, "Indoor visible light communication localization system utilizing received signal strength indication technique and trilateration method," *Opt. Eng.* **57**(1), 016107 (2018), doi: 10.1117/1.OE.57.1.016107.

Indoor visible light communication localization system utilizing received signal strength indication technique and trilateration method

Farag I. K. Mousa,[a,*] Noor Almaadeed,[b] Krishna Busawon,[a] Ahmed Bouridane,[c] Richard Binns,[a] and Ian Elliot[a]
[a]Northumbria University, Department of Mathematics, Physics and Electrical Engineering, Newcastle Upon Tyne, United Kingdom
[b]Qatar University, Department of Computer Science and Engineering, Doha, Qatar
[c]Northumbria University, Department of Computer and Information Sciences, Newcastle Upon Tyne, United Kingdom

Abstract. Visible light communication (VLC) based on light-emitting diodes (LEDs) technology not only provides higher data rate for indoor wireless communications and offering room illumination but also has the potential for indoor localization. VLC-based indoor positioning using the received optical power levels from emitting LEDs is investigated. We consider both scenarios of line-of-sight (LOS) and LOS with non-LOS (LOSNLOS) positioning. The performance of the proposed system is evaluated under both noisy and noiseless channel as is the impact of different location codes on positioning error. The analytical model of the system with noise and the corresponding numerical evaluation for a range of signal-to-noise ratio (SNR) are presented. The results show that an accuracy of <10 cm on average is achievable at an SNR > 12 dB.
[DOI: 10.1117/1.OE.57.1.016107]

Keywords: light-emitting diodes; received optical power; received signal strength indication; localization; indoor positioning; visible light communication; trilateration method.

Paper 171140 received Jul. 21, 2017; accepted for publication Dec. 12, 2017; published online Jan. 9, 2018.

1 Introduction

One of the essential problems of indoor visible light communication (VLC) consists of determining the user location to channel the correct information to the authorized user, thus ensuring both privacy and security. In this context, one might be tempted to use Global Positioning System (GPS) as a technique for determining the user location. Unfortunately, the GPS is not suitable to providing accurate indoor positioning because of strong attenuation of the electromagnetic waves inside buildings as well as high cost.[1] As a result, several approaches using a wireless-fidelity system have been proposed to overcome this problem. However, these techniques result in a lack of accuracy and coverage as well as higher interference problem and installation cost.[1,2] Some of the typical methods of implementing VLC positioning include:

- Time of arrival (TOA): this technique uses signal propagation time to determine the user's position, i.e., it is based on the time for the signal to travel from transmitter to receiver.[3]
- Angle of arrival (AOA): this technique is based on the intersection of several pairs of angle direction lines, each formed by the circular radius between the transmitter and the device's user.[4]
- Time difference of arrival (TDOA): the main idea of TDOA is that the difference between the arriving times between signals from at least three transmitters is used to estimate the user's location.[2]
- Received signal strength indication (RSSI): this method uses the received power levels that are measured at the receiver side (i.e., the received signal strength) to estimate the distances between the transmitters and a receiver.

In addition, there are a number of subtechniques that have been developed, including the positioning algorithm in Ref. 5, where each transmitter has a unique identifier that is a single tone with all of them having a frequency lower than 700 kHz; this is also known as discrete multitone. Moreover, a hybrid positioning method based on range-free VLC together with RSSI is proposed in Ref. 1. In Ref. 6, an RF carrier allocation technique is utilized for an indoor VLC positioning system based on intensity modulation with a direct detection (IM/DD) technique. Furthermore, in Ref. 7, the optical orthogonal code is used in an algorithm with the trilateration method, and an average location error of 0.08 m is obtained. However, the previous works neglected the effect of noise and multipath distortions of the VLC channel. In addition, these works did not calculate the location error for all positions in a standard size room and did not take into account the impulse response of light-emitting diodes (LEDs).[1–3,5,7–15] However, in Ref. 16, the influence of noise was considered, but the signal-to-noise ratio (SNR) was very high (i.e., SNR = 30 dB). On the other hand, in Ref. 17, the non-line-of-sight (NLOS) was considered with very low noise level, i.e., noise power level is −140 to −180 dBmw. In Ref. 18, multipath distortions and the effect of noise were considered, but the SNR was very high (i.e., SNR = 25 dB) and the positioning error was around 1 m. Finally,

*Address all correspondence to: Farag I. K. Mousa, E-mail: farag.mousa@northumbria.ac.uk

0091-3286/2018/$25.00 © 2018 SPIE

in Refs. 19 and 20, the effect of multipath is considered, but the influence of noise is neglected and the localization errors were relatively high. In this paper, we focus on the RSSI technique because it does not need synchronization between the transmitter and the receiver and it is simple.[8] Our aim is to provide a precise estimation of the user's location and derive the performance degradation in a typical room where VLC is implemented. More precisely,

- We design an integrated indoor VLC system end to end, that is, we take into account all the effects arising from resampling process, impulse response of LED, impulse response of photodetector (PD), and channel impulse response.
- We consider two scenarios of the proposed positioning system: the first scenario is line-of-sight (LOS) only and the second is line-of-sight with nonline-of sight (LOSNLOS), i.e., we calculate the effect of first-order reflections on positioning accuracy.
- We did not neglect the effect of noise in the proposed positioning system whereby we add the noise over a wide range of SNR for both scenarios.
- We derive an analytical model for noise impact on positioning accuracy. Furthermore, we calculate the angular errors and horizontal distance errors against SNR.
- We investigate the impact of different positioning codes on positioning accuracy over a wide range of SNR.
- Finally, we calculate and plot the positioning errors by various methods (spatial distribution, estimated and real position, and statistical standards) with and without noise and calculate the average positioning error for the whole typical room against SNR for LOS and LOSNLOS scenarios.

The rest of this paper is organized as follows. In Sec. 2, the VLC channel modeling is presented. Then, the theoretical aspects of the indoor VLC positioning system are given in Sec. 3. In Sec. 4, the mathematical model of the RSSI technique with the trilateration method and mathematical analysis of noise are presented. In Sec. 5, a discussion of the results obtained is made, followed by concluding remarks in Sec. 6.

2 Some Preliminaries—Visible Light Communication Channel Modeling

In this section, we recall some of the basic methodologies for VLC channel modeling that exist in the literature. The general form of the Friis transmission equation gives the relationship between transmitted and received power for any communication system[10]

$$P_{\mathrm{Rx}} = P_{\mathrm{Tx}}.H(L)\cdot G_{\mathrm{Rx}}, \tag{1}$$

where P_{Rx} and P_{Tx} are the received and transmitted signal power, respectively, G_{Rx} is the receiver gain, and $H(L)$ is the channel gain, which is a function of distance L.

The relationship between transmitted and received optical power is written as follows:

$$P_{\mathrm{Rx}} = \sum_i \left(P_{\mathrm{Tx}_i} h_{\mathrm{ch,LOS}_i}(t) + \int_{\mathrm{walls}} P_{\mathrm{Tx}_i} \mathrm{d}h_{\mathrm{ch,NLOS}_i}(t) \right), \tag{2}$$

where i is the index of the i'th transmitter, LOS stands for the line-of-sight, and NLOS refers to the nonline-of-sight paths (also referred to as the diffused configurations). In this work, we distinguish two cases: (i) LOS and (ii) LOSNLOS. For the first LOS case, the impulse response of VLC channel is expressed as[21,22] in

$$h_{\mathrm{ch,LOS}_i}(t) = \begin{cases} \frac{1}{L_i^2} R_{o,\mathrm{LOS}}(\theta) A_{\mathrm{eff,LOS}}(\psi) \delta\left(t - \frac{Li}{c}\right) & 0 \le \psi \le \mathrm{FOV} \\ 0 & \text{otherwise} \end{cases}, \tag{3}$$

with

$$R_{o,\mathrm{LOS}}(\theta) = \frac{(m+1)}{2\pi}\cos^m(\theta),$$

$$A_{\mathrm{eff,LOS}}(\psi) = A_R\ \cos(\psi) T_S(\psi) g(\psi),$$

where $R_{o,\mathrm{LOS}}(\theta)$ is the transmitter radiant intensity for the LOS scenario, $A_{\mathrm{eff,LOS}}(\psi)$ is the effective signal collection for the LOS scenario, θ is the irradiance angle, ψ is the incidence angle, $T_s(\psi)$ is the gain of an optical filter, $g(\psi)$ is the gain of an optical concentrator, A_R is the detector effective area, $L_i = d(\mathrm{Tx}_i, \mathrm{Rx})$ is the distance between i'th transmitter and the receiver Rx, FOV is the field of view of the receiver, and m is the Lambertian emission, which is given as

$$m = \frac{-\ln(2)}{\ln(\cos(\theta_{1/2}))}, \tag{4}$$

with $\theta_{1/2}$ being the semiangle at half luminance of the LED. On the other hand, in the second NLOS case, the impulse response of VLC channel is given as

$$h_{\mathrm{ch,NLOS}_i}(t) = \begin{cases} \frac{1}{L_{1_{ij}}^2 L_{2_{ij}}^2} R_{o,\mathrm{NLOS}}(\theta_{r_{ij}}) A_{\mathrm{eff,NLOS}}(\psi_{ij}) \mu \delta\left[t - \frac{(L_{1_{ij}} + L_{2_{ij}})}{c}\right] & 0 \le \psi \le \mathrm{FOV} \\ 0 & \text{otherwise} \end{cases}. \tag{5}$$

with

$$R_{o,\mathrm{NLOS}}(\theta_{r_{ij}}) = \frac{(m+1)}{2\pi}\cos^m(\theta_{r_{ij}}),$$

$$A_{\mathrm{eff,NLOS}}(\psi_{r_{ij}}) = A_R\ \cos(\psi_{r_{ij}}) T_S(\psi_{r_{ij}}) g(\psi_{r_{ij}}),$$

$$\mu = \frac{\rho dA_{\mathrm{wall}}}{\pi}\cos(\alpha_{r_{ij}})\cos(\beta_{r_{ij}}).$$

The last term μ is based on Fresnel reflection coefficients, where μ is the factor that gives the effect of the first reflection, $R_{o,\mathrm{NLOS}}(\theta_{r_{ij}})$ is the transmitter radiant intensity for the NLOS scenario, $A_{\mathrm{eff,NLOS}}(\psi)$ is the effective signal collection for the NLOS scenario, i is the index of the i'th transmitter, j is the index of the j'th of multipath, ρ is the reflectance factor, dA_{wall} is a reflective area of small region, L_1 is the distance between LED and a reflective point, L_2 is the distance between a reflective point and a receiver, α_r is

the angle of irradiance to a reflective point, and β_r is the angle of irradiance to the receiver from multipath as shown in Fig. 1.

3 Indoor Visible Light Communication Positioning System Considered

Throughout this paper, we consider the indoor VLC environment as shown in Fig. 2(a).The coordinator, the visible LEDs, and the smart device as a mobile user are three main parts as required in the protocol of IEEE 802.15.7.[8] The standard room size is 5×5 m^2 with height 3 m, and the receiver plane is 0.75 m above floor as shown in Figs. 1 and 2(a). The room is assumed to be empty. The coordinator generates different location codes for all transmitters based on the transmitters' positions. These location codes are combined with the transmitted data (i.e., to frame). The frame is modulated using on–off keying-time division multiplexing (OOK-TDM). The IM/DD was employed to generate the transmitted signal, $x(t)$, as shown in Fig. 2(b).

Notations: In what follows, we shall use the following notations.

- $h_{\mathrm{LED}}(t)$: the impulse response of LED.
- $h_{\mathrm{ch}}(t)$: the impulse response of VLC channel.
- $h_{\mathrm{ch,LOS}_i}(t)$: the impulse response of VLC channel in LOS scenario.
- $h_{\mathrm{ch,NLOS}_i}(t)$: the impulse response of VLC channel in reflection or NLOS scenario.
- $h_{\mathrm{ch,LOSNLOS}_i}(t)$: the impulse response of VLC channel in LOS and NLOS scenario.
- h_{PD}: the impulse response of the PD.
- $n(t)$: an additive white Gaussian noise (AWGN).

The impulse response of an LED, $h_{\mathrm{LED}}(t)$, was derived by applying a pulse function to the LEDs in the lab as shown in Fig. 3(a). As a result, the output signal, $y(t)$, of the LED is given as

$$y(t) = x(t) \circledast h_{\mathrm{LED}}(t) = \int_0^{\infty} x(t-\tau) h_{\mathrm{LED}}(\tau) \mathrm{d}\tau, \tag{6}$$

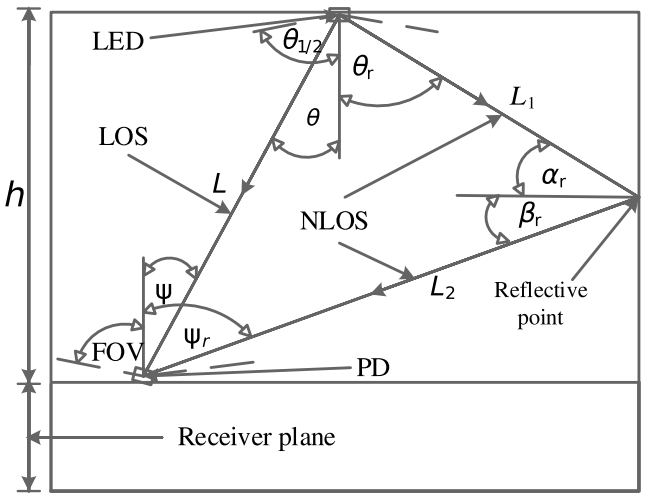

Fig. 1 VLC channel modeling for direct and diffused links.

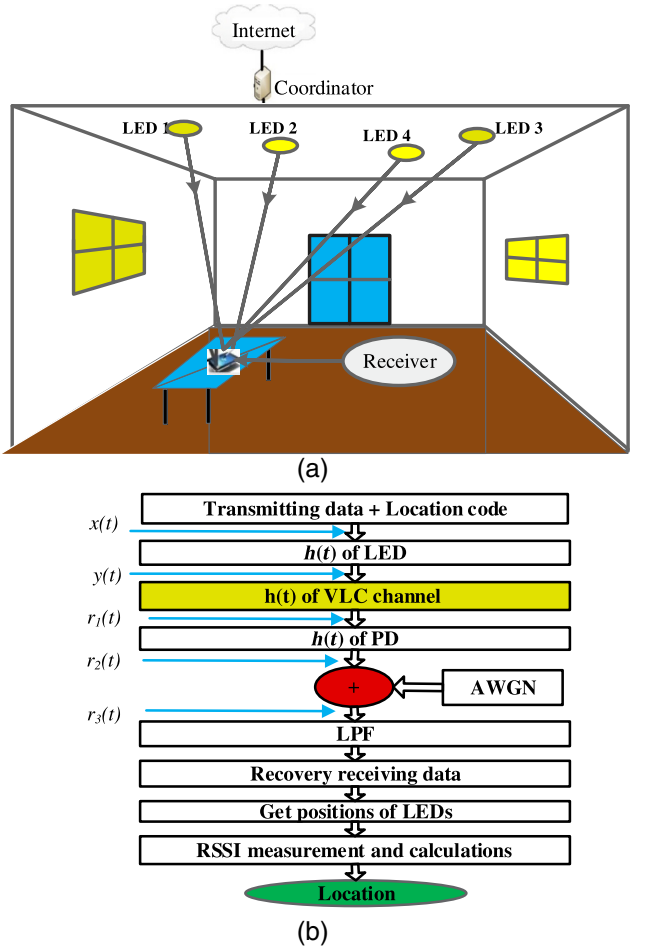

Fig. 2 (a) Indoor VLC positioning system and (b) block diagram of indoor VLC positioning system.

where $\circledast$ denotes the convolution process. Then, the output signal, $y(t)$, is sent to the VLC channel with the impulse response, $h_{\mathrm{ch}}(t)$, as shown in Figs. 3(b) and 3(c). Figure 3(b) shows the impulse response of VLC channel in a LOS scenario, $h_{\mathrm{ch,LOS}_i}(t)$, whereas Fig. 3(c) shows the impulse response of VLC channel in an NLOS scenario $h_{\mathrm{ch,NLOS}_i}(t)$, where we considered only the first reflections. The signal $r_1(t)$ in front of the PD is

$$r_1(t) = y(t) \circledast h_{\mathrm{ch}}(t) = \begin{cases} y(t) \circledast h_{\mathrm{ch,LOS}_i}(t) & \text{for LOS case} \\ y(t) \circledast h_{\mathrm{ch,LOSNLOS}_i}(t) & \text{for LOSNLOS case} \end{cases}. \tag{7}$$

At the receiver side, the output of the PD is

$$r_2(t) = r_1(t) \circledast h_{\mathrm{PD}}(t), \tag{8}$$

where $h_{\mathrm{PD}} =$ constant. In this work, we assume $h_{\mathrm{PD}} = 0.6$. Ultimately, the received signal of the overall system is expressed as

$$r_3(t) = r_2(t) + n(t), \tag{9}$$

where $n(t)$ is the background noise, which is the combination of thermal, shot, and dark noise and can be modeled as additive white Gaussian noise (AWGN).

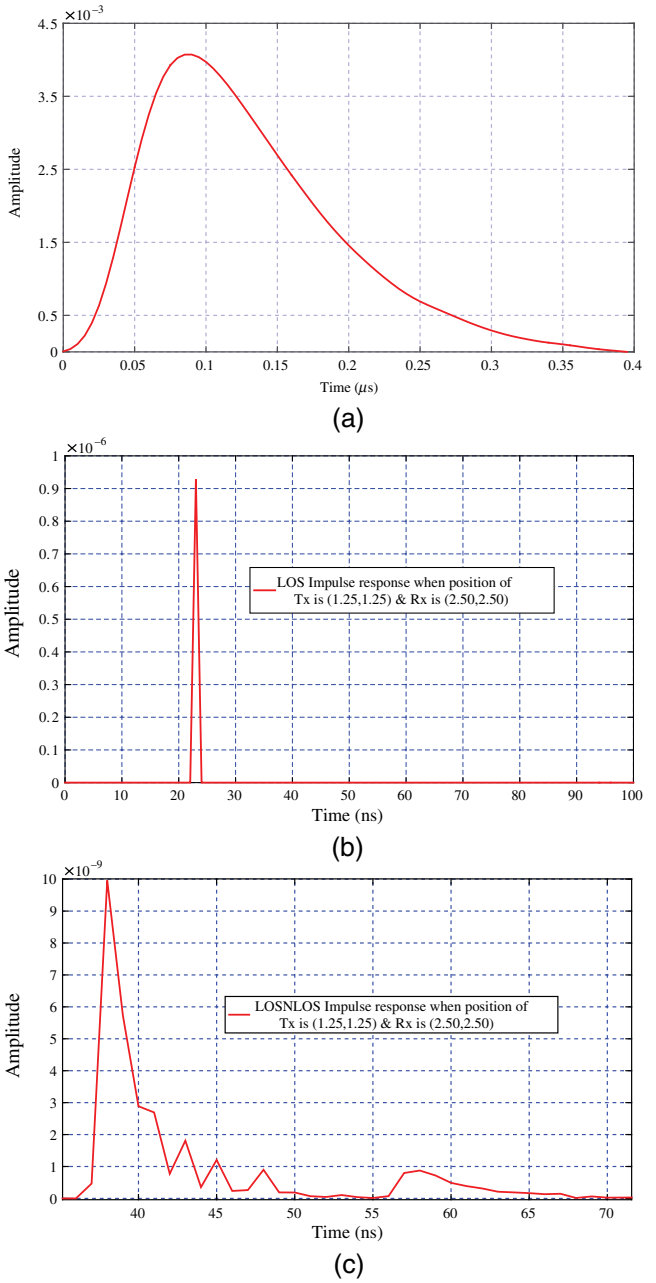

Fig. 3 Impulse responses of VLC positioning system: (a) the LED impulse response, (b) an impulse response of VLC channel for LOS scenario, and (c) an impulse response of VLC channel for NLOS.

A low-pass filter (LPF) was used to reduce the impact of noise. The RSSI technique was implemented to obtain the user's location. Using this technique, the receiver separates the received data from each transmitter by slot time and recovers the original data with location codes. These location codes were then used to detect the locations of the transmitters and simultaneously measure the power level for every LED $[P_{\mathrm{Rx},L_i}(\theta_{L_i})]$. Consequently, we obtain the received optical power $P_{\mathrm{Rx},V}(0)$ at distance V from the typical room measurements. Finally, by applying the RSSI algorithm and the trilateration method, we obtain the user's location. In Sec. 4, the user's location methodology will be explained. The flow of the mathematical and signal process is shown in Fig. 2(b).

4 User Location Methodology Using RSSI Technique

This section discusses the RSSI technique of indoor positioning using three transmitters with the trilateration method. This approach recovers channel characteristics from incident light and estimates the receiver location by analytically solving the Lambertian equation group. In what follows, we describe the algorithm that allows us to calculate the path loss as a result of attenuation. From Eq. (2), which is a basic equation that calculates the received power in the VLC environment for any location inside a room, the received power at a distance L_i utilizing Eqs. (2) and (3) is expressed as follows:

$$P_{\mathrm{Rx},L_i}(\theta_{L_i},\psi_{L_i}) = P_{\mathrm{Tx}_i}\frac{(m+1)}{2\pi L_i^2}\cos^m(\theta_{L_i})T_s(\psi_{L_i})g_s(\psi_{L_i})\cos(\psi_{L_i}). \tag{10}$$

The received power underneath the transmitter, i.e., at distance V and $\psi_{L_i} = \theta_{L_i} = 0$, is given as

$$P_{\mathrm{Rx},V}(0,0) = P_{\mathrm{Tx}_i}\frac{(m+1)}{2\pi V^2}, \tag{11}$$

as shown in Fig. 4. From Eqs. (10) and (11), assuming $T_s(\psi).g_s(\psi) = 1$ and $\psi_{L_i} = \theta_{L_i}$, the mathematical model of the RSSI technique is written as

$$P_{\mathrm{Rx},L_i}(\theta_{L_i},\theta_{L_i}) = P_{\mathrm{Rx},V}(0,0)\cos^{(m+\gamma+1)}(\theta_{L_i}), \tag{12}$$

where $i = 1, 2, 3$, or 4 represents the number of transmitters in the room and $\gamma = 2$ is a path-loss exponent correction factor.[5,23] In the sequel, we shall rewrite Eq. (12) as

$$P_{\mathrm{Rx},L_i}(\theta_{L_i}) = P_{\mathrm{Rx},V}(0)\cos^{(m+\gamma+1)}(\theta_{L_i}), \tag{13}$$

for the sake of simplicity.

4.1 *Horizontal Distance Estimation*

From Eq. (13), one calculates the angle of irradiance (θ_{L_i}) using the measurements of the received power at distance V and the received power at distance L_i. We now calculate the horizontal distance estimation, d_{L_i}, as[23]

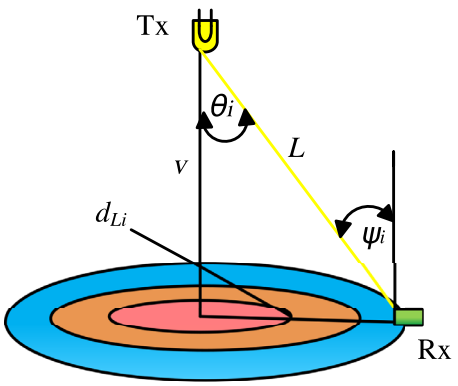

Fig. 4 Side view of one-dimensional indoor VLC system.

$$d_{L_i} = V \tan(\theta_{L_i}). \tag{14}$$

4.2 *Trilateration Method*

The process of determining absolute or relative locations of targets by measuring the distances using the geometry of circles is shown in Fig. 5. Therefore, there are four power levels to be measured at the receiver side. However, the receiver will only select the three maximum power levels that will be used by the positioning algorithm to determine the location of the user. Thus, we use the RSSI algorithm to calculate θ_{L_i} (i.e., θ_{L_1}, θ_{L_2}, and θ_{L_3}). We then calculate d_{L_1}, d_{L_2}, and d_{L_3} using Eqs. (13) and (14), respectively. Now, the trilateration method is used to determine the position of the user by obtaining the intersection point from the three following equations:

$$\begin{cases} (x_{\mathrm{Rx}} - x_{\mathrm{Tx}_1})^2 + (y_{\mathrm{Rx}} - y_{\mathrm{Tx}_3})^2 = d_{L_1}^2 \\ (x_{\mathrm{Rx}} - x_{\mathrm{Tx}_2})^2 + (y_{\mathrm{Rx}} - y_{\mathrm{Tx}_2})^2 = d_{L_2}^2 \\ (x_{\mathrm{Rx}} - x_{\mathrm{Tx}_3})^2 + (y_{\mathrm{Rx}} - y_{\mathrm{Tx}_3})^2 = d_{L_3}^2 \end{cases}, \tag{15}$$

where d_{L_1}, d_{L_2}, and d_{L_3} are the horizontal distances between transmitters and receiver and $(x_{\mathrm{Tx}_1}, y_{\mathrm{Tx}_1})$, $(x_{\mathrm{Tx}_2}, y_{\mathrm{Tx}_2})$, and $(x_{\mathrm{Tx}_3}, y_{\mathrm{Tx}_3})$ are the position coordinates of the transmitters, where $(x_{\mathrm{Rx}}, y_{\mathrm{Rx}})$ is the position of the receiver.

4.3 *Mathematical Analysis of Noise*

In this section, we develop a noise analysis for the proposed positioning system. By setting, $k = m + \gamma + 1$, Eq. (13) is then rewritten as

$$P_{\mathrm{Rx},L_i}(\theta_{L_i}) = P_{\mathrm{Rx},V}(0).\cos^k(\theta_{L_i}). \tag{16}$$

The above equation expresses the ideal system case, which means there is no noise affecting the system. From this, we derive

$$\theta_{L_i} = \cos^{-1}\left[\sqrt[k]{\frac{P_{\mathrm{Rx},L_i}(\theta_{L_i})}{P_{\mathrm{Rx},V}(0)}}\right]. \tag{17}$$

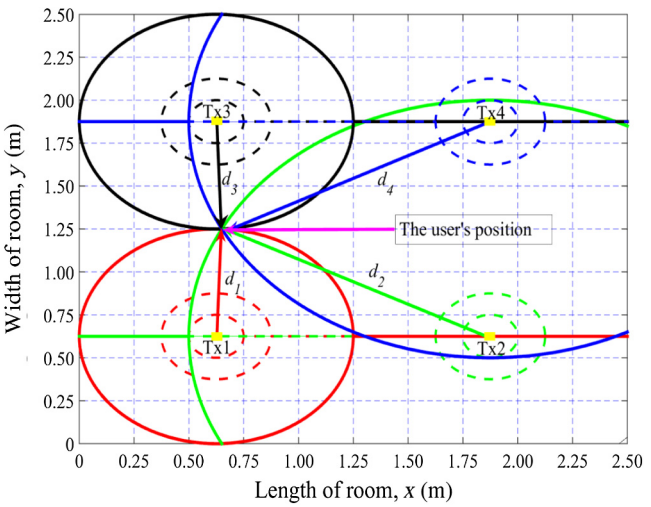

Fig. 5 Top view of two-dimensional (2-D) positioning system.

On the other hand, in the presence of noise, we have

$$\{P_{\mathrm{Rx},L_i}(\theta_{L_i}) + P_{n_i}\} = \{P_{\mathrm{Rx},V}(0) + P_{n_o}\}\cos^k(\theta_{L_i} + \Delta\theta_{L_i}), \tag{18}$$

where P_{n_i} and P_{n_o} are the noise power levels at distance L_i and V, respectively, both obeying white Gaussian distribution. Consequently

$$\theta_{L_i} + \Delta\theta_{L_i} = \cos^{-1}\left[\sqrt[k]{\frac{P_{\mathrm{Rx},L_i}(\theta_{L_i}) + P_{n_i}}{P_{\mathrm{Rx},V}(0) + P_{n_0}}}\right], \tag{19}$$

that is

$$\Delta\theta_{L_i} = \cos^{-1}\left[\sqrt[k]{\frac{P_{\mathrm{Rx},L_i}(\theta_{L_i}) + P_{n_i}}{P_{\mathrm{Rx},V}(0) + P_{n_0}}}\right] - \cos^{-1}\left[\sqrt[k]{\frac{P_{\mathrm{Rx},L_i}(\theta_{L_i})}{P_{\mathrm{Rx},V}(0)}}\right], \tag{20}$$

and the link *snr* is given by

$$snr = \frac{P_{\mathrm{Rx},L_i}(\theta_{L_i})}{P_{n_i}} \Leftrightarrow P_{n_i} = \frac{P_{\mathrm{Rx},L_i}(\theta_{L_i})}{snr}, \tag{21}$$

where the *snr* is the linear value of signal-to-noise ratio. Then, $\Delta\theta_{L_i}$ is rewritten as

$$\Delta\theta_{L_i} = \cos^{-1}\left[\sqrt[k]{\frac{P_{\mathrm{Rx},L_i}(\theta_{L_i})[1 + 1/snr]}{P_{\mathrm{Rx},V}(0)}}\right] - \cos^{-1}\left[\sqrt[k]{\frac{P_{\mathrm{Rx},L_i}(\theta_{L_i})}{P_{\mathrm{Rx},V}(0)}}\right]. \tag{22}$$

From Eq. (14), we calculate the horizontal distance error in the ideal case whereas the real case is given as

$$d_{L_i} + \Delta d_i = V \tan(\theta_{L_i} + \Delta\theta_{L_i}), \tag{23}$$

$$\Delta d_i = V\{\tan(\theta_{L_i} + \Delta\theta_{L_i}) - \tan(\theta_{L_i})\}. \tag{24}$$

Finally, from Eqs. (22) and (24), we obtain the relationship between the angular error $(\Delta\theta_{L_i})$ or the horizontal distance error (Δd_i) and SNR at any point in the VLC room.

5 Results and Discussions

5.1 *Test Parameters*

The indoor positioning system was simulated using MATLAB® to pinpoint the user's position. We considered a resampling process to reduce the effect of noise and channel distortion on the location codes that have information of the transmitters' positions. These location codes are necessary to the positioning algorithm, so we obtain acceptable bit error rates (BERs). The system parameters are presented in Table 1.

Table 1 Simulation parameters for the proposed VLC positioning system.

Parameters	Values
Size of room: Length × Width × Height	5 m × 5 m × 3 m
Number of LED-based transmitters	4
Transmitters locations	As in Fig. 5
The LED's semiangle at half power (FWHM)	70 deg
Transmitted power (per transmitter)	10 W
LED bandwidth	3 MHz
Transmit data rate R_B	5 Mbps
Receiver plane above the floor	0.75 m
PD type	OSD-15T
Active area (A_R) of receiver	50×10^{-6} m^2
PD responsivity	0.6
Half angle FOV of receiver	80 deg
Detector orientation: tilt horizontal (elevation)	0 deg
Detector orientation: tilt vertical (azimuth)	0 deg
PD O/E conversion efficiency	0.6 A/W
Receiver sensitivity (used with the AD8015 transimpedance amplifier)	−36 dBm
LPF cutoff frequency	R_BMHz
X-Y sweep resolution (*m*)	0.25 × 0.25

5.2 *Results and Discussion*

First of all, the location algorithm, which is shown in Fig. 2(b), is applied to obtain the performance of the location error at 441 points on the receiver plane in a typical room (5 m × 5 m × 3 m) by the two scenarios mentioned before (i.e., LOS and LOSNLOS). Because we assumed that the difference in the received optical power levels (i.e., the positioning errors) between two positions (i.e., the distance between them is <25 cm) is very small, it can be ignored. The second reason is that we tested 25 positions per square meter as a real scenario that is enough to evaluate the performance of proposed positioning system. According to Ref. 24, the required SNR to achieve a target BER of 10^{-6} is 13.6 dB. Therefore, our simulation will consider an SNR of more than 13.6 dB. From the mathematical analysis of noise, we simulated and plotted the relationship between the angular error ($\Delta\theta$) and a wide range of SNR when the receiver is located at different positions of the room as shown in Fig. 6(a), where we select three different positions. It is noted that the angular error is different from one position to another when the SNR is <10 dB. However, it has approximately the same effect when the SNR is high. The relationship between the horizontal distance error (Δd) and SNR is plotted in Fig. 6(b) for three different positions of the receiver where it can be seen that the horizontal distance error becomes stable at higher SNR > 20 dB.

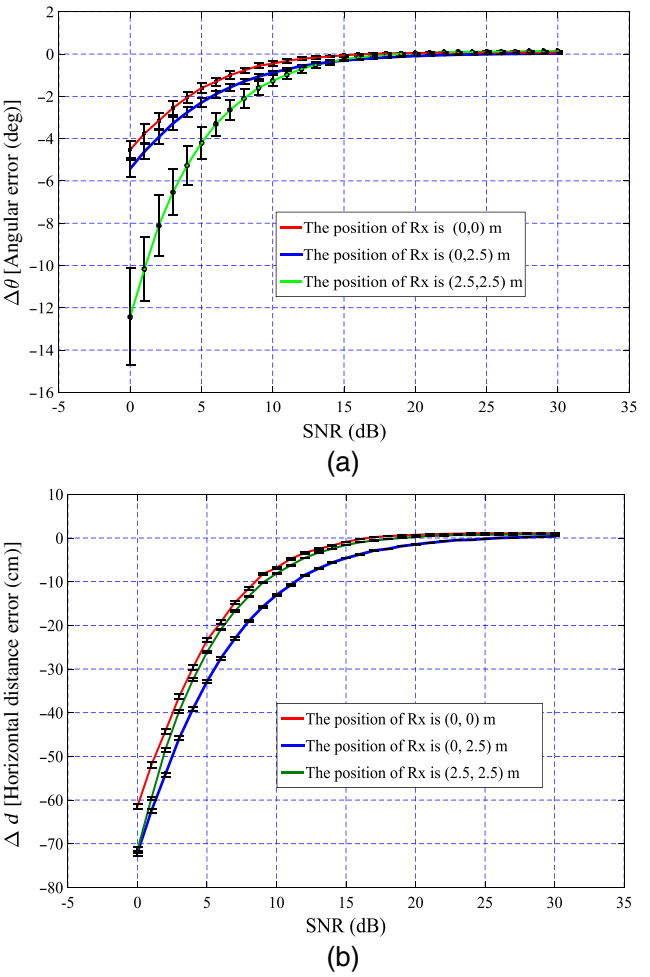

Fig. 6 The relationship between SNR and average and variance bar for (a) angular error ($\Delta\theta_{L_i}$) and (b) horizontal distance error (Δd_{L_i}).

In this section, we investigate the effect of different location codes on the angular error and the horizontal distance error. We assume four different location codes as a binary stream, which are {00000001}, {10000000}, {10101010}, and {11111111}. This means that every signal has different average power levels, which are 0.125, 0.125, 0.50, and 1, respectively, as normalized power. It is worth noting that there is a difference among location codes when the SNR is lower than 15 dB but a similar effect on both the angular error or the horizontal distance error when the SNR is higher than 15 dB as shown in Figs. 7(a) and 7(b). Therefore, we conclude that there is not any impact on the positioning accuracy when we use different location codes with OOK modulation. In the first scenario, the positioning system is considered an ideal system meaning that noise is not taken up at any stage in the aforementioned VLC system. The results are based on two different procedures that are LOS in the absence of any reflections from walls. In the second procedure, we consider both the LOS and NLOS (LOSNLOS), which are shown in Figs. 8(a) and 8(b), respectively. Furthermore, all statistical measures (mean, standard deviation, and maximum) indicate that there is a free error in the LOS procedure as in Fig. 8(a). However, in the second procedure, the average error has increased in all locations in the typical room, especially

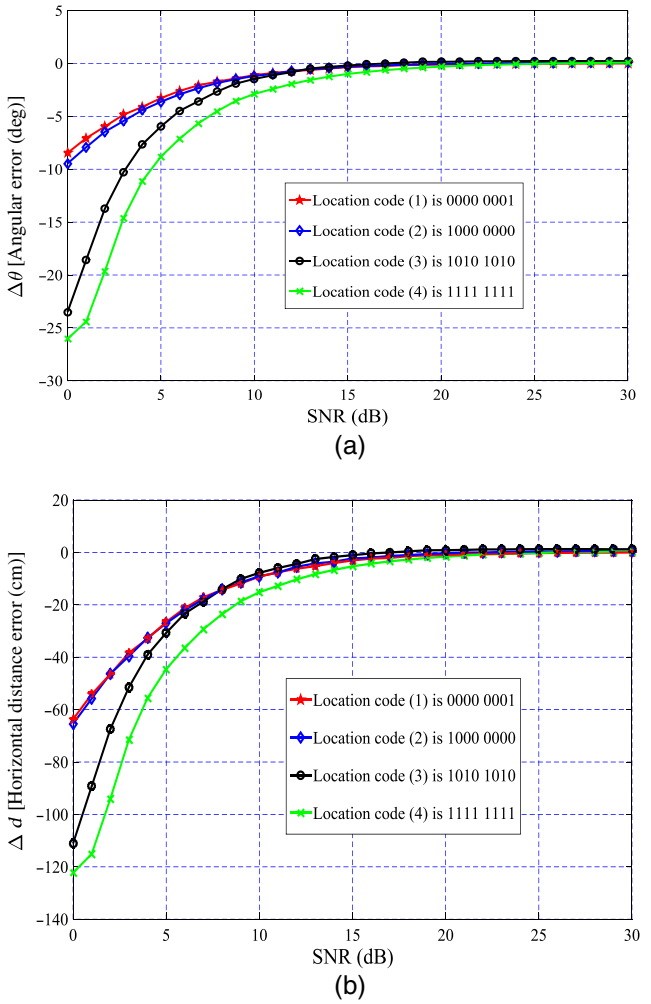

Fig. 7 The relationship between SNR and average (a) angular error $(\Delta\theta_{L_i})$ and (b) horizontal distance error (Δd_{L_i}) for different location codes when the position of receiver is (2.5, 2.5) m.

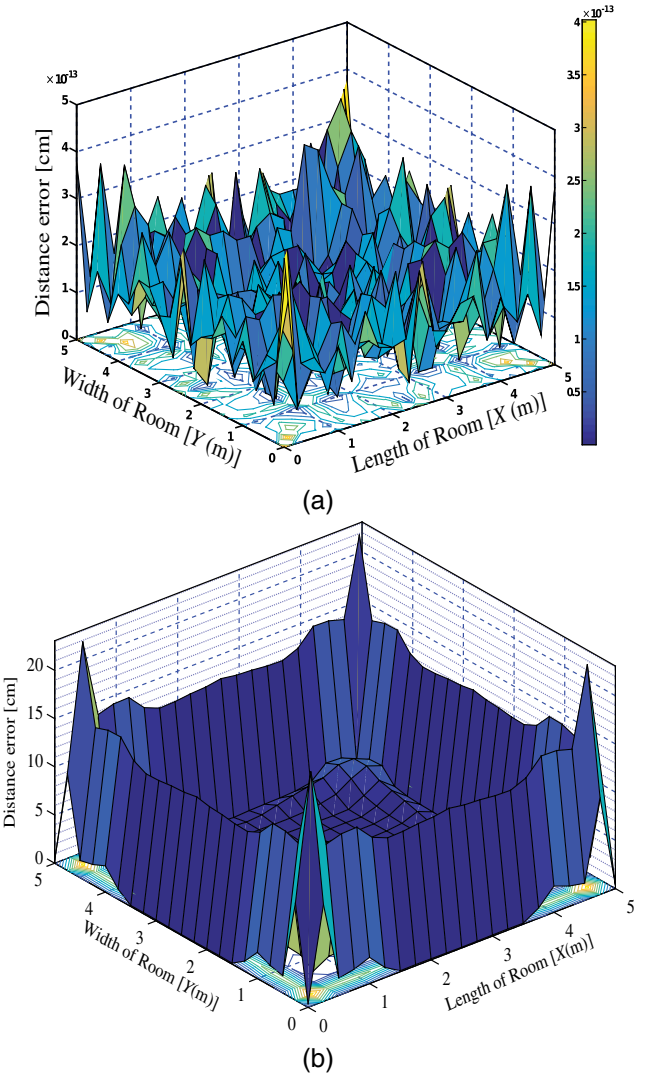

Fig. 8 Spatial distribution of localization error for ideal system: (a) LOS scenario and (b) LOSNLOS scenario.

near the walls, where the maximum and average positioning error are 20 and 3.5 cm, respectively, because of the directionality of the Lambertian. This means that there are strong reflections near the walls while in the middle of the room, and the positioning error is very low because of the reflections are very weak. On the mathematical side, in the LOSNLOS scenario, we performed a convolution process between the transmitted signal from LED and the impulse response of the LOSNLOS channel, which has a large number of symbols. However, in the LOS scenario, we used a multiplication process between the transmitted signal from LED and the impulse response of the LOS channel that has only one symbol. Finally, it is to be noted that Figs. 8(a) and 8(b) show the impact of the reflections from the LOSNLOS scenario and the significant difference between LOS and LOSNLOS scenarios in the case of strong reflections.

In the second scenario, we further investigate the case when noise is present. In Fig. 2(b), we added noise $n(t)$ into the received optical signal $r_2(t)$ as shown in Eq. (9) using *awgn function* from MATLAB® (i.e., which is modeled as a normal Gaussian distribution (AWGN) over the SNR range of 0 to 30 dB). The same positioning algorithm is applied here, and the same previous scenarios, which are LOS and LOSNLOS, are also considered. The selected localization error distributions as well as the real and estimated positions are plotted at 15 dB and are shown in Figs. 9(a), 9(b), 10(a), and 10(b), respectively. It is to be noted that there is some difference in Figs. 10(a) and 10(b) where one observes that the majority of the estimated positions are inside the room. Therefore, it is a useful feature, and we note that the effect of reflections is clear on the estimated positions that are close to walls. In addition, some statistical measures (mean, standard deviation, and maximum) are shown in Table 2 that explains that the localization error average decreases spectacularly when SNR increases. Note that Figs. 9(a), 9(b), 10(a), and 10(b) relate to the statistical measures shown in Table 2 when SNR = 15 dB. We compared the two scenarios when the system is noiseless and noisy as shown in Figs. 8 and 9, respectively. From this comparison, note that the noise effects on positioning error for the LOS scenario in Fig. 9(a) when SNR = 15 dB, and the positioning error is free in the absence of noise as shown in Fig. 8(a). Therefore, there is a significant effect of noise in the proposed positioning system. The same effect occurs for LOSNLOS scenario as is shown in Figs. 8(b) and 9(b).

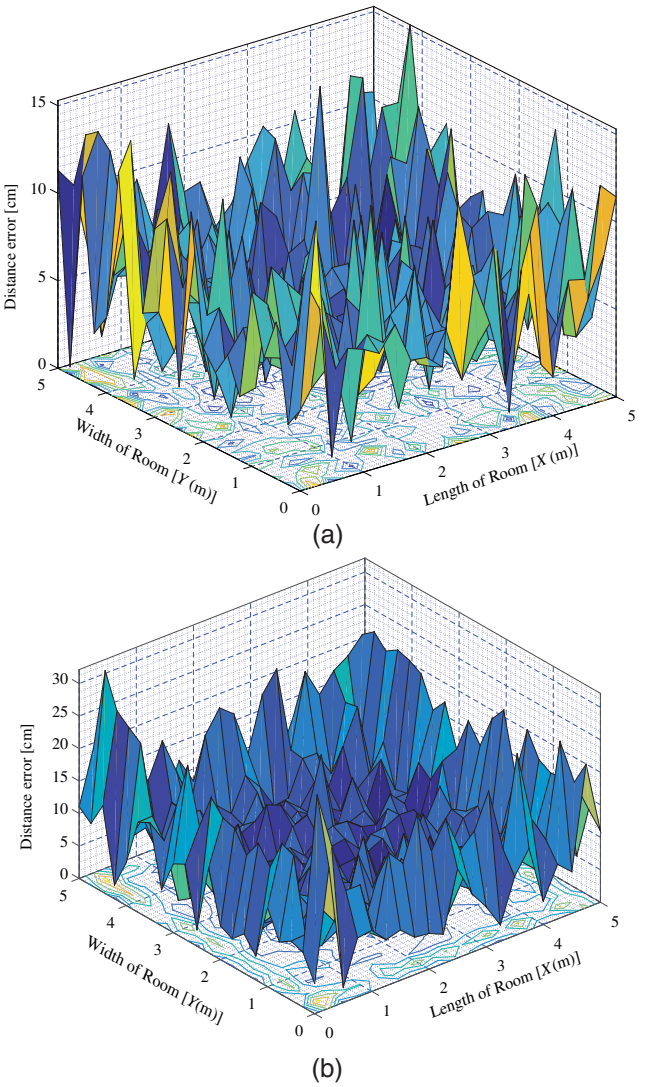

Fig. 9 Spatial distribution of localization error for real system at SNR = 15 dB: (a) LOS scenario and (b) LOSNLOS scenario.

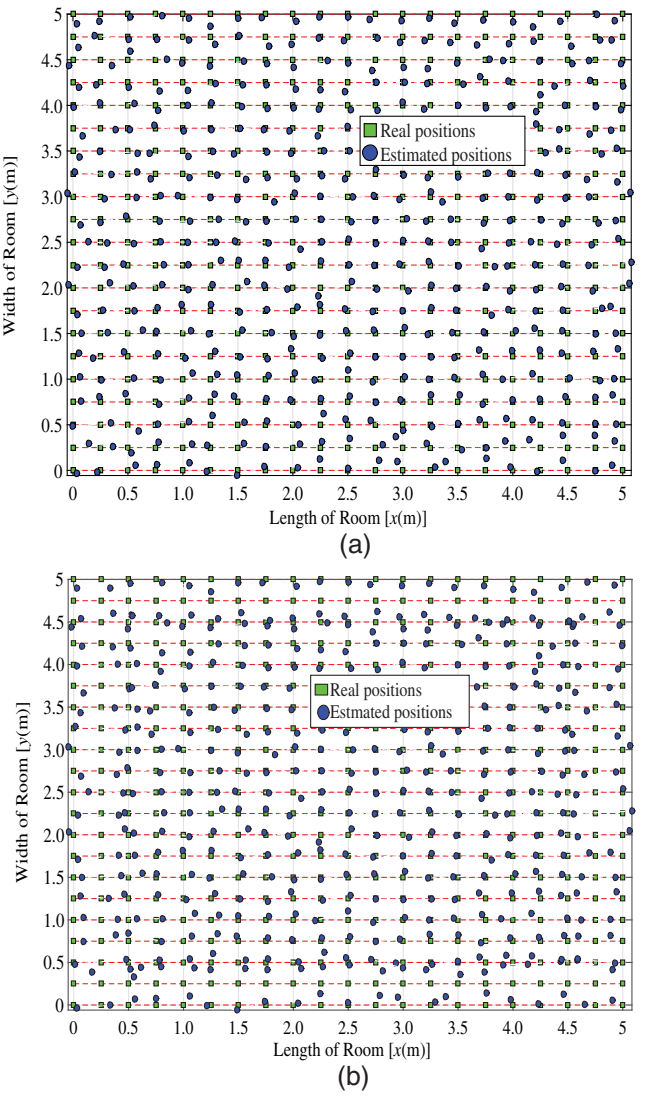

Fig. 10 Estimated (green square) and real positions (blue circle) for real system at SNR = 15 dB: (a) LOS scenario and (b) LOSNLOS scenario.

Moreover, Fig. 11 shows the average of all positioning errors in the room against a wide range of SNR values for LOS and LOSNLOS scenarios. Indeed, both scenarios provide an average error which is <7 cm when SNR = 15 dB. On the other hand, at an SNR of ∼30 dB, LOS scenario provides an average error that is close to zero whereas the average error in LOSNLOS scenario is <5 cm. This is due to the directionality of Lambertian and the impact of noise. Indeed, we assumed that the room is empty, but the proposed system can be given in some cases in a real room, such as if the receiver is near something inside room (e.g., a person). In this case, we consider it is to be the same as if the receiver is near a wall if there is no blocking and the positioning error will be <21.76 and 32.15 cm when SNR is more than 15 dB for LOS and LOSNLOS scenarios, respectively. However, if it is a little remote from the wall or something, the proposed positioning system will be able to work as in a normal case. Furthermore, if one transmitter is blocked by something, then the proposed system can work efficiently because it depends on three transmitters and the model has four transmitters. However, if two transmitters are blocked, the positioning error will be high.

5.3 *Comparative Analysis of the Results*

To evaluate the proposed positioning system, in which the same RSSI technique and trilateration method are used, a comparison of the results with other works in the literature is required. For a fair comparison, the same conditions under which the results in the previous works were conducted were also used in the proposed study (for instance, the VLC environment and modulation scheme parameters as shown in Table 3). The summary in Table 3 is divided into two scenarios: an LOS scenario and an LOSNLOS scenario. Each scenario has two cases: noisy and noiseless. Note that, in the noiseless LOS scenario, error free positioning is obtained in our study while this is not the case in the previous studies. On the other hand, in the noisy LOS scenario, the results in the previous works show the positioning accuracy only at specific values instead over a range of SNR. For instance, in Refs. 16 and 26, the accuracies are given only at an

Table 2 The statistical standards for LOS and NLOS scenarios of the proposed VLC positioning system.

SNR (dB)	Maximum (cm)	Mean (cm)	Standard deviation (cm)
	LOS scenario		
0	103.57	53.45	20.57
5	61.09	26.62	12.62
10	33.23	11.59	6.24
15	21.76	5.61	3.25
20	12.67	2.97	1.82
25	5.61	1.63	0.97
30	2.57	0.90	0.50
	LOSNLOS scenario		
0	117.35	54.72	22.24
5	80.97	29.23	14.66
10	46.53	14.50	9.00
15	32.15	8.05	6.00
20	28.51	5.28	5.29
25	24.76	4.21	5.24
30	23.56	3.56	5.20

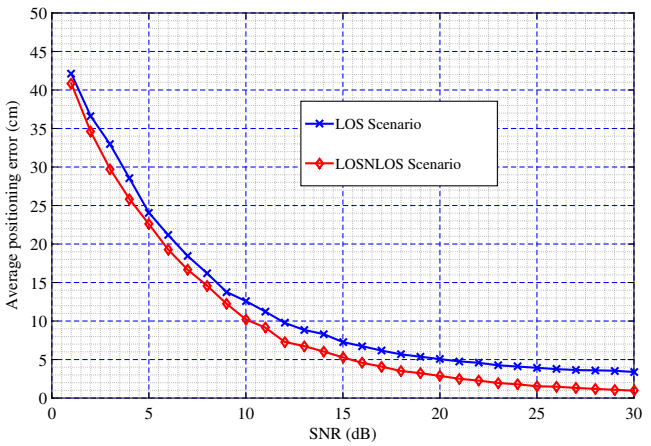

Fig. 11 The relationship between positioning error average against SNR for real-positioning system.

SNR of 30 and 15 dB, which were found to be 5 and 10 cm, respectively.

In the noiseless LOSNLOS scenario, the previous results show that the average positioning error is high; for example, in Refs. 19 and 20, the errors are 0.8064 m and 14.98 cm, respectively, whereas in the proposed positioning system, the average distance error is <3.5 cm. On the other hand, in the noisy LOSNLOS scenario, the average positioning error was 0.5 mm in Ref. 17, but the noise power was very low (i.e., the range of noise power is from −140 to −180 dBm). In addition, in Ref. 27, the RMS error was 1.01 m when SNR = 25 dB. However, in our work, the average distance error is 4.21 cm when SNR is 25 dB. At the end of this comparison, we conclude that the proposed positioning system as investigated in LOS and LOSNLOS scenarios under both noisy and noiseless cases is more comprehensive with the highest accuracy reported so far.

Table 3 The comparison of the RSSI techniques in the VLC positioning system.

Author's name	Ref	Typical room	Modulation	Noise	Average error
		LOS scenario			
Yang et al.	14	$90\times90\times150$ cm^3	NRZ-OOK	No	1.575 cm
Gu et al.	25	$6\times6\times3.5$ m^3	OOK	No	0.0464 m
Zhang and Kavehrad	16	$6\times6\times4$ m^3	OOK	30 dB	≈5 cm
Lim	26	$6\times6\times4$ m^3	OOK	15 dB	10 cm
		LOSNLOS scenario			
Gu et al.	19	$6\times6\times3.5$ m^3	OOK	No	0.8064 m
Elkarim et al.	20	$5\times5\times4$ m^3	Not sp.	No	14.98 cm
Zhou et al.	17	$3\times3\times3$ m^3	RZ-OOK	−140 dBm	0.5 mm
Aminikashani et al.	18 and 27	$6\times6\times3.5$ m^3	OOK	25 dB	1.01 m

Note: Not sp. = not specified.

6 Conclusions

This paper discussed a 2-D indoor positioning system using LED ceiling lamps that are modeled mathematically using an RSSI technique. The simulations were carried out to calculate the effect of distortions of the received optical power from three transmitters using the trilateration method. We found that there is no effect on the positioning accuracy when different location codes are used. The proposed positioning algorithm is able to determine the user's location with an average error of 5 cm when SNR is 15 dB for the LOS system. However, the error average in the LOSNLOS is around 8 cm when SNR is equal to 15 dB. In general, the average error decreases dramatically when SNR is increased over 15 dB. Finally, a comparison is made with previous works on the subject, and we have demonstrated good performance of the proposed positioning scheme.

References

1. J. Ziyan, "A visible light communication based hybrid positioning method for wireless sensor network," in *Second Int. Conf. on Intelligent System Design and Engineering Application (ISDEA)*, pp. 1367–1370 (2012).
2. J. Soo-Yong et al., "TDOA-based optical wireless indoor localization using LED ceiling lamps," *IEEE Trans. Consum. Electron.* **57**, 1592–1597 (2011).

3. T. Q. Wang et al., "Position accuracy of time-of-arrival based ranging using visible light with application in indoor localization systems," *J. Lightwave Technol.* **31**, 3302–3308 (2013).
4. M. S. Islam et al., "Indoor positioning through integration of optical angles of arrival with an inertial measurement unit," in *Position Location and Navigation Symp. (PLANS)*, pp. 408–413 (2012).
5. G. Cossu et al., "A visible light localization aided optical wireless system," in *IEEE GLOBECOM Workshops (GC Workshops)*, pp. 802–807 (2011).
6. K. Hyun-Seung et al., "An indoor visible light communication positioning system using a RF carrier allocation technique," *J. Lightwave Technol.* **31**, 134–144 (2013).
7. S. Yamaguchi et al., "Design and performance evaluation of VLC indoor positioning system using optical orthogonal codes," in *IEEE Fifth Int. Conf. on Communications and Electronics (ICCE)*, pp. 54–59 (2014).
8. T. Nguyen et al., "Highly accurate indoor three-dimensional localization technique in visible light communication systems," *J. Korea Inst. Commun. Sci.* **38C**, 775–780 (2013).
9. C. Sertthin et al., "6-axis sensor assisted low complexity high accuracy-visible light communication based indoor positioning system," *IEICE Trans. Commun.* **E93-B**(11), 2879–2891 (2010).
10. P. H. Liqun et al., "Epsilon: a visible light based positioning system," in *Proc. of the 11th USENIX Conf. on Networked Systems Design and Implementation (NSDI)*, pp. 331–343 (2015).
11. Y. Hu et al., "Lightitude: indoor positioning using ubiquitous visible lights and COTS devices," in *IEEE 35th Int. Conf. on Distributed Computing Systems (ICDCS)*, pp. 732–733 (2015).
12. W. Yong-Yuk et al., "Three-dimensional optical wireless indoor positioning system using location code map based on power distribution of visible light emitting diode," *IET Optoelectron.* **7**, 77–83 (2013).
13. G. B. Prince et al., "A two phase hybrid RSS/AoA algorithm for indoor device localization using visible light," in *IEEE Global Communications Conf. (GLOBECOM)*, pp. 3347–3352 (2012).
14. S. H. Yang et al., "Visible light based high accuracy indoor localization using the extinction ratio distributions of light signals," *Microwave Opt. Technol. Lett.* **55**, 1385–1389 (2013).
15. H. Swook et al., "White LED ceiling lights positioning systems for optical wireless indoor applications," in *36th European Conf. and Exhibition on Optical Communication (ECOC)*, pp. 1–3 (2010).
16. W. Zhang and M. Kavehrad, "A 2-D indoor localization system based on visible light LED," in *IEEE Photonics Society Summer Topical Meeting Series*, pp. 80–81 (2012).
17. Z. Zhou, M. Kavehrad, and P. Deng, "Indoor positioning algorithm using light-emitting diode visible light communications," *Opt. Eng.* **51**, 085009 (2012).
18. M. Aminikashani et al., "Indoor location estimation with optical-based OFDM communications," 2015, https://pdfs.semanticscholar.org/b177/61ffa459e946c403d0d86aff2d34dfe8c2db.pdf (December 2017).
19. W. Gu et al., "Multipath reflections analysis on indoor visible light positioning system," 2015, https://pdfs.semanticscholar.org/aed9/dc337bb35cfd4c1d7a50d6f87441ed34eccb.pdf (December 2017).
20. M. Elkarim, N. Mohammed, and M. Aly, "Exploring the performance of indoor localization systems based on VLC-RSSI, including the effect of NLOS components using two light-emitting diode lighting systems," *Opt. Eng.* **54**, 105110 (2015).
21. Z. Ghassemlooy, W. O. Popoola, and S. Rajbhandari, *Optical Wireless Communications—System and Channel Modelling with MATLAB*, CRC Press, Boca Raton, Florida (2012).
22. S. Dimitrov and H. Haas, *Principles of LED Light Communications: Towards Networked Li-Fi*, Cambridge University Press, Cambridge (2015).
23. F. I. K. Mousa et al., "Indoor localization system utilizing two visible light emitting diodes," *Opt. Eng.* **55**, 116114 (2016).
24. T. Komine et al., "Fundamental analysis for visible-light communication system using LED lights," *IEEE Trans. Consum. Electron.* **50**, 100–107 (2004).
25. W. Gu et al., "Three-dimensional indoor light positioning algorithm based on nonlinear estimation," *Proc. SPIE* **9772**, 97720V (2016).
26. J. Lim, "Ubiquitous 3D positioning systems by led-based visible light communications," *IEEE Wireless Commun.* **22**, 80–85 (2015).
27. M. Aminikashani et al., "Indoor positioning in high speed OFDM visible light communication," 2015, https://pdfs.semanticscholar.org/3100/bde8c342c3f3f6533739cdcdbb346dc30cb9.pdf (December 2017).

Farag I. K. Mousa received his BSc degree in electrical and computer engineering from Nasser University, Al-khums, and his MSc degree in communication and waves from the High Studies Academy, Tripoli, Libya, in 2001 and 2008, respectively. He was a lecturer at Nasser University for four years. He has published six scientific papers. He is currently working toward his PhD and studying positioning and cryptography in visible light communication (VLC) system at Northumbria University, United Kingdom.

Noor Almaadeed is an assistant professor in the Computer Science and Engineering Department, Qatar University. In 2014, she received her PhD in computer science and engineering from Brunel University. She graduated from the Qatar Leadership Centre, first batch 2013. She has been a lecturer of computer engineering at Qatar University since 2001. Her areas of research are speech signal detection, speaker identification, and audio/visual speaker recognition. She was awarded Qatar Education Excellence Award, 2015.

Krishna Busawon is a professor in control systems engineering and is currently the head of Nonlinear Control Research Group, the Faculty of Engineering and Environment, Northumbria University. He obtained his PhD in control systems engineering from University Lyon I in 1996. His recent research interests are in chaos and optical wireless communications, hybrid systems, and the area of mathematical modeling, nonlinear control, and estimation. He is currently the principal investigator of a number of PhD students.

Ahmed Bouridane received his Ingenieur d'Etat degree in electronics from ENPA, Algeria, in 1982, and his PhD in computer vision from Nottingham University, United Kingdom, in 1992. He joined Queen's University, Belfast, in 1994 and was promoted to Reader in 2000. He is now a professor of computer science and leads Computer and Electronic Security Systems, Northumbria University, Newcastle. His research interests are in information security and communications. He has published more than 350 publications. He is a SM'05 of IEEE.

Richard Binns received his PhD in analogue test strategies from Huddersfield University in 1997. He worked on an EPSRC postdoctoral contract in collaboration with Ericson Components and Cadence Design Systems. He is the head of the Department of Mathematics Physics and Electrical Engineering, Northumbria University, United Kingdom, and established collaborative links to institutions in Malaysia, Singapore, and China. Current research works are varied from the design of electronics for VLCs and energy management in electric vehicles.

Ian Elliott has been a lecturer in higher education for over 25 years, teaching a wide range of subjects in the electronics. He held a BSc (honors) and an MPhil in electrical and electronic engineering. He published several research papers and textbook. He is teaching a considerable number of graduate and under-graduate students of digital system design, his current interests include advanced hardware description, verification languages, mixed-signal design and modelling.